Journal Pre-proof

Influence of processing conditions on microstructural, mechanical and tribological properties of graphene nanoplatelet reinforced UHMWPE

M.J. Martínez-Morlanes, F.J. Pascual, G. Guerin, J.A. Puértolas

PII: S1751-6161(20)30787-6

DOI: https://doi.org/10.1016/j.jmbbm.2020.104248

Reference: JMBBM 104248

To appear in: *Journal of the Mechanical Behavior of Biomedical Materials*

Received Date: 2 October 2020

Revised Date: 27 November 2020

Accepted Date: 29 November 2020

Please cite this article as: Martínez-Morlanes, M.J., Pascual, F.J., Guerin, G., Puértolas, J.A., Influence of processing conditions on microstructural, mechanical and tribological properties of graphene nanoplatelet reinforced UHMWPE, *Journal of the Mechanical Behavior of Biomedical Materials* (2021), doi: https://doi.org/10.1016/j.jmbbm.2020.104248.

María José Martínez-Morlanes: Investigation, Writing- Original draft preparation, Writing- Reviewing and Editing. **Francisco Javier Pascual**: Investigation, Visualization, Writing- Original draft preparation, Writing- Reviewing and Editing. **Gautier Guerin:** Investigation. **José Antonio Puertolas:** Conceptualization, Investigation, Funding acquisition, Supervision, Writing- Original draft preparation, Writing- Reviewing and Editing.

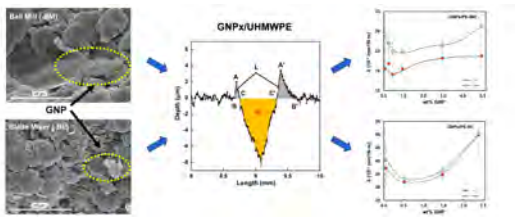

Influence of processing conditions on microstructural, mechanical and tribological properties of graphene nanoplatelet reinforced UHMWPE

M.J. Martínez-Morlanes[1], F.J. Pascual[2], G. Guerin[1], J.A. Puértolas[1*]

[1]Department of Materials Science and Technology, Instituto de Investigación en Ingeniería de Aragón, I3A, Universidad de Zaragoza, 50018 Zaragoza, Spain

[2]Centro Universitario de la Defensa de Zaragoza, Academia General Militar, Zaragoza 50090, Spain

*Correspondence to Prof. José A. Puértolas

Department of Materials Science and Technology,

Escuela de Ingeniería y Arquitectura-I3A, Universidad de Zaragoza,

E-50018, Zaragoza, Spain

Tel.: +34 976 762521

Fax.: +34 976 761957

e-mail:japr@unizar.es

ABSTRACT

Ultra-high molecular weight polyethylene (UHMWPE) is a relevant thermoplastic in industry and a well-proven standard biomaterial in joint replacements. To enhance its tribological properties while preserving its bulk ones, composite coatings on a UHMWPE substrate were prepared using non-functionalised graphene nanoplatelet (GNP) at reinforcement concentration of 0.1 to 5 wt% and two mechanical mixing techniques (ball mill or blade mixer) with different consolidation temperatures of 175 to 240 °C. Changes in morphology and size of the UHMWPE particles before hot-pressing were observed in function of the mechanical mixing techniques applied. Wear rate was affected by graphene content, reaching a minimum at 0.5 wt% GNP, with a reduction of 20 and 15 %, for ball milling and blade mixer, respectively. However, blade mixer increased the wear rate by around twice respect the ball milling results, for all the studied materials. The coefficient of friction decreased notably, by ~25%, below 3 wt% GNP content, and hardness increased by 24%, regardless of the mechanical mixing process used. Finally, consolidation temperature had a positive influence on wear rate at temperatures of around 195 °C, which could be related to the free radical scavenger effect of the GNP.

KEYWORDS: Wear resistance; polymer-matrix composite; graphene nanoplatelets; polyethylene; hardness; particle shape.

1. INTRODUCTION

Ultra-high molecular weight polyethylene (UHMWPE) is a semi-crystalline, hydrophobic polymer with remarkably high mechanical properties, tribological performance and chemical stability due mainly to its long polymer chains, which link the lamella of the polymer. On the other hand, its biocompatibility makes it suitable for medical applications, UHMWPE being considered one of the most attractive materials for total joint replacement (Kurtz 2016).

Nonetheless, to enhance its properties and to develop new applications, this polymer has been combined with various micro and nanofillers: W, TiB_2, B_4C or Sm_2O_3 for protection against neutron, X-ray, cosmic, electron or gamma radiation; and MoS_2, kaolin, Al_2O_3, glass or ZnO as solid lubricants to optimise its tribological behaviour for industrial applications (Puértolas and Kurtz, 2016). Further, self-reinforced composites (UHMWPE fibres) have been produced for use in ballistic protection, industrial and consumer applications (Siskey et al., 2016).

One of the key factors that determines the properties of composites is the intrinsic characteristics of the fillers, particularly their shape, size, morphology and surface area. Currently, graphene and other carbonaceous materials, such as reduced graphene oxide (RGO), graphene oxide (GO), graphene oxide nanosheets (GONs) and graphene nanoplatelets (GNPs) or nanosheets (GNS), which meet filler requirements, hold great promise for advancements in this field. They have exceptional properties including a high aspect ratio, elastic modulus, thermal conductivity and performance as a solid lubricant, besides their new quantum effects and electro-optical behaviour (Berman et al., 2016; Lee et al., 2008; Zhu et al., 2018), all these being modulated as a function of the specific number of layers stacked in the particle.

The high viscosity of UHMWPE in a molten state due to its high molecular weight (of nearly 2-6 Mg/mol) precludes the use of fabrication methods commonly employed in the production of other polymer matrix composites. In this case, the preparation method consists of blending of the filler and the polyethylene powder, followed by hot thermoforming. The initial step provides a graphene-coated UHMWPE powder, which does not ensure an even distribution of the graphene in the resulting composite, but rather a segregated structure. This latter type of filler distribution is highly suitable for producing polymer composites with a low electrical resistivity and a low percolation threshold, provided that the filler is conductive (Maruzhenko et al., 2019; Wang et al., 2013). However, it limits the space occupied by the graphene layers, favouring the formation of aggregates by van der Waals interactions between the graphene particles, and consequently, strongly affecting the mechanical and tribological properties of the composite (Puértolas and Kurtz, 2014; Tripathi, 2017).

Seeking to minimise the adverse influence of the segregated structure, various procedures have been assessed, such as solvent (water or ethanol)-assisted dispersion followed by the reduction of GONs with hydrazine (Pang et al., 2012), reduction of GO (Hu et al., 2018), and ultrasonication in alcohol of GNS or GNP (Alam et al., 2019; Aliyu et al., 2020; Du et al., 2011;Wang et al., 2018). With the aim of avoiding the toxicity and carcinogenic risks of the reducing agents, other techniques have been developed, for example, based on dry-mixing by mechanical methods, electrostatic adsorption combined with a high-speed stirring process (Wang et al., 2013) or use of a mortar (Al-Saleh, 2017; Maruzhenko et al., 2019). The aforementioned dry methods, with no use of solvents or functionalisation of the filler, not only significantly reduce production costs but also open the way to potential applications in strictly regulated sectors such as the biomedical field.

Dry blending can affect mechanical and thermal performance via various mechanisms. Specifically, modifications in the morphology of GNP particles can alter their lower aspect ratio and decrease their ability to transfer load from the matrix as well as their lubricating properties. Further, changes in the relative position of the graphene at the interface with the UHMWPE particles can affect the adhesion between the composite coating and the substrate. On the other hand, these mechanical processes may also influence the UHMWPE particle size, and the presence of graphene as well as the consolidation temperature may alter the polymer chain mobility between the UHMWPE grains producing changes in the oxidation processes. To the best of our knowledge, all these mechanisms remain poorly understood and warrant research due to their importance in the final macroscopic properties of the composites.

Therefore, the aim of this study was to prepare GNP/UHMWPE composite coatings with different filler loadings using two different mechanical dry-blending methods, in order to study the influence of these methods on the tribological properties. In addition, we have also investigated the influence of the consolidation temperature during the compression moulding on the wear resistance of these composites. Finally, we have explored the association between these results and morphological characteristics of the graphene-coated polymer powders provided by the different manufacturing process.

2. MATERIAL AND METHODS

2.1 Materials

Medical grade UHMWPE (GUR® 1050) in powder form was supplied by Celanese, USA, with an average particle size of 150 μm and a molecular weight of 8.6 million

g/mol and without additives. AvanPLAT-40® multilayer GNPs obtained by mechanical exfoliation of graphite were purchased from Avanzare, Spain. These GNPs take the form of around 10-nm thick multilayer structures (≤30 layers) with a lateral platelet size of 40 µm.

2.2 Composite consolidation

UHMWPE powder was blended with GNPs at concentrations of 0.1, 0.3, 0.5, 1, 3 or 5 wt% for coating purposes. The mixture was homogenised in a ball mill for 8 hours at 400 rpm to obtain an even distribution of the filler in the polymer matrix, following a procedure used in previous work (Chih et al., 2017).With the aim of studying the influence of the blending process, coatings were also prepared using a blade mixer with GNP concentrations of 0.5, 1.4, 2.3 or 4.6 wt%. The powder mixtures were carefully deposited onto the surface of a pre-formed virgin UHMWPE disk (Ø = 90 mm), previously compressed to 10 MPa at room temperature for 10 minutes. The composite layer and the substrate were then thermo-compressed together in a heated platen press (Specac, UK), at 175 °C under a constant pressure (10 MPa) for 30 min followed by air-cooling under the same pressure. In order to study the influence of compression moulding temperature, composite coatings with 1 and 5 wt% GNP content were pressed at 195, 220 and 240 °C. These consolidation temperatures are conventional for commercial grades of UHMWPE intended for biomedical applications (Kurtz et al., 1999). Furthermore, the upper limit of the temperature region is chosen in order to minimise fusion defects (Gao and Mackley 1994, Wu et al., 2002) and improve ductility (Fu et al., 2010). Furthermore, The final composite materials consisted of a composite layer around 0.5 mm thick held in a 3.5-mm layer of neat PE. Composites were referred to as PE (raw material), GNPx/PE-BM-T (composites made using a ball mill) and

GNPx/PE-BL-T (those made using a blade mixer), x being the weight percentage of the filler and T the consolidation temperature. If the temperature is not specified, the sample was made at 175 °C.

2.3 Physicochemical characterisation

Fourier-transform infrared (FTIR) spectroscopy was performed to analyse the chemical composition of the surface of the composites. The measurements were carried out in a Vertex 70 spectrometer (Bruker, Germany). Consolidated surfaces were measured in an attenuated total reflectance configuration, while the FTIR spectra of the GNPs in powder form were obtained using pressed disks of the solid combined with KBr, and measured in a transmission configuration. The spectra were obtained with a resolution of 4 cm^{-1} and by the accumulation of 32 spectra between 4000 and 500 cm^{-1}.

Morphological analysis was conducted on both samples, in powder form and on freeze-fractured surfaces, previously coated with gold using a sputtering device (Balzers SCD-4, Switzerland) to make a conductive surface on the sample. The samples were observed with a Gemini field emission scanning electron microscope (Carl Zeiss, Switzerland) in the secondary electron mode at 5 keV with a probe current of 100 pA. Raman spectra were measured on the surface of the coating with a Horiba Jobin Yvon Raman spectrometer HR 800 UV (Horiba, Japan), using a 532 nm laser.

2.4 Microhardness

Vickers hardness was measured with a digital micro-hardness tester MXT70 (Matsuzawa Co., Japan). A standard Vickers indenter was used with a load of 25 g and an indentation time of 15 s. The tests were carried on cylindrical samples with a

diameter of 6 mm. The mean value of at least ten measurements and the corresponding standard deviation were calculated in each sample for each material.

2.5 Tribological tests

A commercial ball-on-disk tribometer (CSM Instruments, Switzerland) allowed the measurement of the wear resistance and coefficient of friction (COF) for all materials, according to ASTM G99-17. Wear tests were performed on rotating disks with a diameter of 20 mm, a thickness of 3 mm and a surface roughness of 0.39 ± 0.06 μm immersed in deionised water (used as a lubricant) and the environmental temperature was kept at 37 °C. The counterpart, pressed against the rotating disk, was a stationary alumina ball (6 mm in diameter, Ra = 0.050 ± 0.002 μm) mounted in a pin specially designed for this test geometry. The applied load was 5 N, resulting in a Hertzian contact pressure of 37 MPa, which is in the range of peak contact stresses for some PE components commonly used in total knee replacements (Lewis, 1998; Szivek et al., 1996). Frictional force in the pin is internally calculated by the tribometer software from the data registered by two inductive displacement transducers. Consequently, the COF, also denoted as μ, is calculated by dividing the frictional force into the applied load of 5 N. The COF, was monitored for 24 h with a sliding speed of 0.05 m/s, which corresponds to a sliding distance of 4320 m as the diameter of the circular track was 4 mm. After each tribometer test (n=1), worn disk surfaces were evaluated by confocal microscopy using a SENSOFAR Plμ-2300 optical imaging profiler. The worn areas identified were used to calculate the wear rate, k, using the following equation: $k = V_m/F \cdot s$, where F is the perpendicularly applied load, s the sliding distance and V_m the worn volume given by $V_m = 2\pi r A_m$ where r is the wear track radius and A_m the average

worn area. The area was the mean of four track profiles, which were obtained in two diametrically opposite directions on each studied sample.

3. RESULTS AND DISCUSSION

3.1 Morphology of the powder

Figure 1 shows the morphology of the as-supplied UHMWPE powder. These particles are spheroid in shape with a broad range of diameters from around 40 to 200 mm (Figure 1a). The single particles were observed to have a hierarchical so-called “cobweb” structure. Inside the grains, bundles of fibrillary elements are seen linking subparticles of material resembling nodules (Olley et al., 1999). A lumpy structure dominates on the surface, partially covering the particles, allowing the aforementioned interconnected structure to be seen at some points (Figures 1b-c).

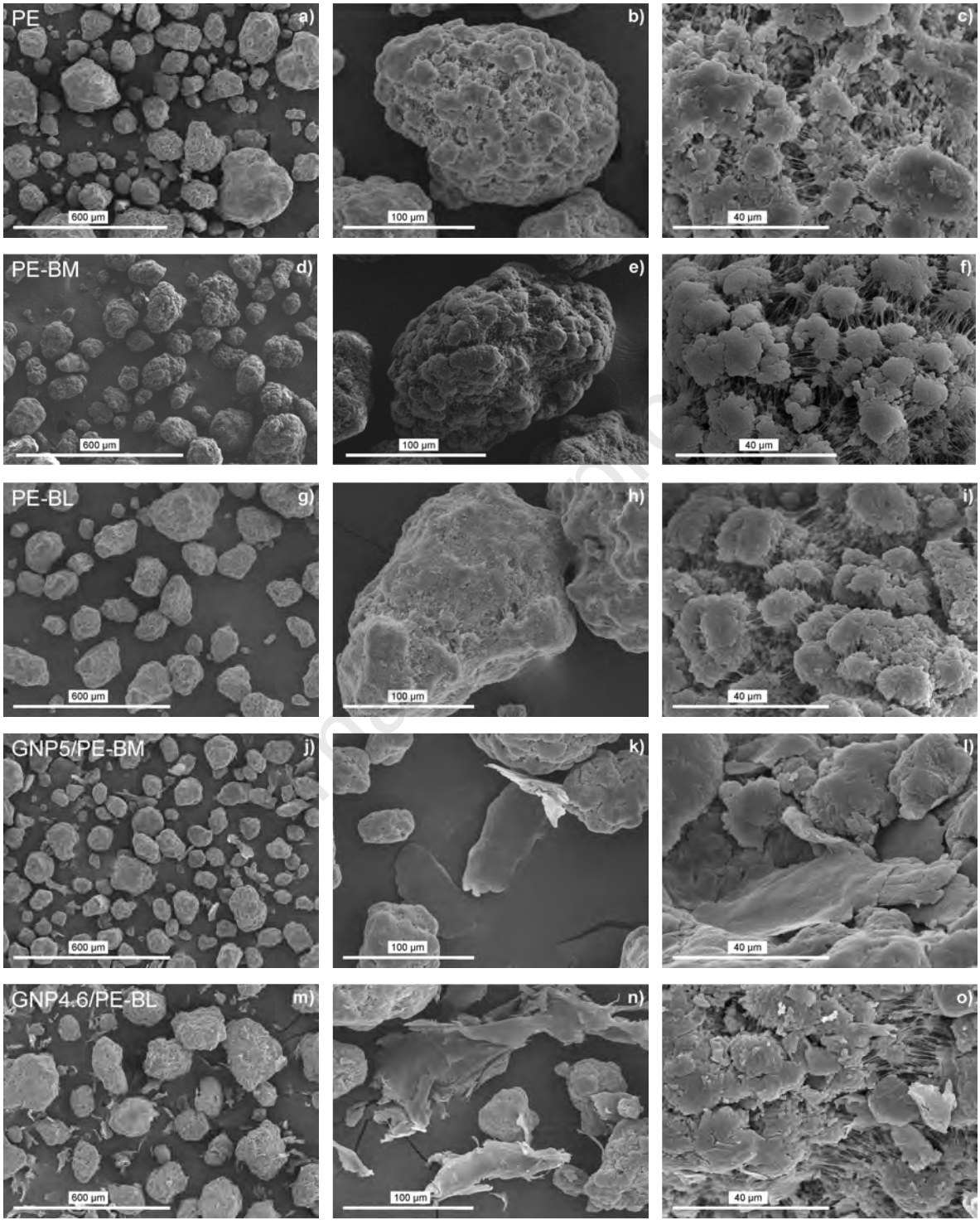

Figure 1. Scanning electron microscopy images of different powders studied at different magnification scales: (a-c) neat polyethylene (PE) as supplied, (d-f) neat PE after ball mill mixing, (g-i) neat PE after blade mixing technique, and (j-l) the composites at 5 wt% obtained using a ball mill (at 5 wt%) or (m-o) a blade mixer (at 4.6 wt%).

The distribution of neat PE particles after ball milling (PE-BM) and blade mixing (PE-BL) is shown in Figures 1d and 1g, respectively. The former technique did not change the size of the PE particles but did modify their surface. The lumpy morphology appears over a more extended area, probably due to the plastic deformation produced by the impact of the steatite balls during milling (Figures 1e-f). In contrast, the blade mixing technique influences the external morphology less (Figures 1h-i), probably due to the shear stress on particles during the process, but on the other hand, increases the size of the particles, unlike the impact of ultrasonication (Liu et al., 2016) or high rpm during ball milling (Suñer and Emami, 2014) in which the particles are fragmented.

Figures 1j and 1m also indicate that the two mechanical mixing methods, using a ball mill and blade mixer respectively, have different effects on the graphene particles. Firstly, the PE particles are thickened during the blade mixer process, while during ball milling, they retain their initial size.

Regarding to the composite powders, SEM images reveal the presence of GNP layers outside the polymer grains after both methods (Figure 1k and 1n). However, it can be seen that the GNP layers keep their shape after ball milling, while the graphene has a flayed morphology when the blade mixer is used.

Also, the presence of GNP on the surface of polymer grains is also affected by the mixing technique. Thus, after ball milling, the GNPs seem to be flaked on the surface of the grains (Figure 1l), while after the blade mixing technique the GNPs are mainly near of the voids in the fibrillary structure of the polymer (Figure 1o).

In any case, the observation of several particles indicates that even at the highest filler concentration, although the presence of graphene was detected on the surface of grains,

it does not fully coat them, differing with the findings of Wang et al. (2013). This difference could be associated with the size of the graphene particles, ours being of 40 μm, much larger than the 0.5-1 μm particles used in their study.

3.2 Physicochemical surface characterisation

FTIR measurements were performed to check for the presence of GNPs as well as evaluate possible changes in surface crystallinity of graphene composite coatings after the consolidation process. Figure 2a shows the spectra obtained for as-received GNP powder, neat PE and GNPx/PE-BM composites thermo-compressed at 175 °C. It can be seen that the main infrared (IR) signals corresponding to the GNPs are the C=C stretching in the aromatic ring at 1576 cm^{-1} and the peaks at 1632 cm^{-1} and 3443 cm^{-1} which correspond to the O-H modes of adsorbed water. Additionally, the IR spectrum for thermo-compressed PE showed the characteristic absorption bands for the methylene C-H asymmetric/symmetric stretching at 2918 and 2849 cm^{-1}, respectively, methylene C-H bending at 1462 cm^{-1} and methylene $–(CH_2)_n-$ rocking at 719 cm^{-1} (Coates, 2000). Regarding the composite coatings, all of them showed the bands associated with both bare PE and the graphene modes, regardless of the mixing technique used. The temperature increase up to 240 °C did not produce significant surface changes respect to the presence of GNP in any the materials studied (Figure 2b).

Furthermore, it is known that crystallinity can influence the wear resistance of composites as we will discuss later. Given this, FTIR spectral analysis was also used to carry out a qualitative assessment of the surface crystallinity of the consolidated materials. This analysis is based on the intensity ratio of the methylene bending bands at 1473 and 1463 cm^{-1}, which is known to be inversely related to crystallinity values (Zerbi et al., 1989). The results shown in Figure 2c indicate a significant decrease in the

intensity ratio up to 1% GNP loading for -BM and 2 wt% for the -BL composites, suggesting an increase in the surface crystallinity. Similar results were found in the study of Alam et al.(2019) in which the degree of crystallinity of UHMWPE reached a maximum at 1 wt% GNP content. On the other hand, increasing the compression moulding temperature had different effects depending on the GNP concentration (Figure 2c). Thus, for neat PE, the increase of this temperature up to 240ºC resulted in a higher intensity ratio reflecting a decrease in crystallinity. A similar effect, although much stronger, was also observed for the GNP1/PE-BM coating; however, the trend changed at the highest GNP loading (5 wt%), where the intensity ratio decreased, indicating an increase in surface crystallinity of this composite coating. This difference could be related to the nucleating effect of GNPs during re-crystallisation, which might be amplified at higher temperatures.

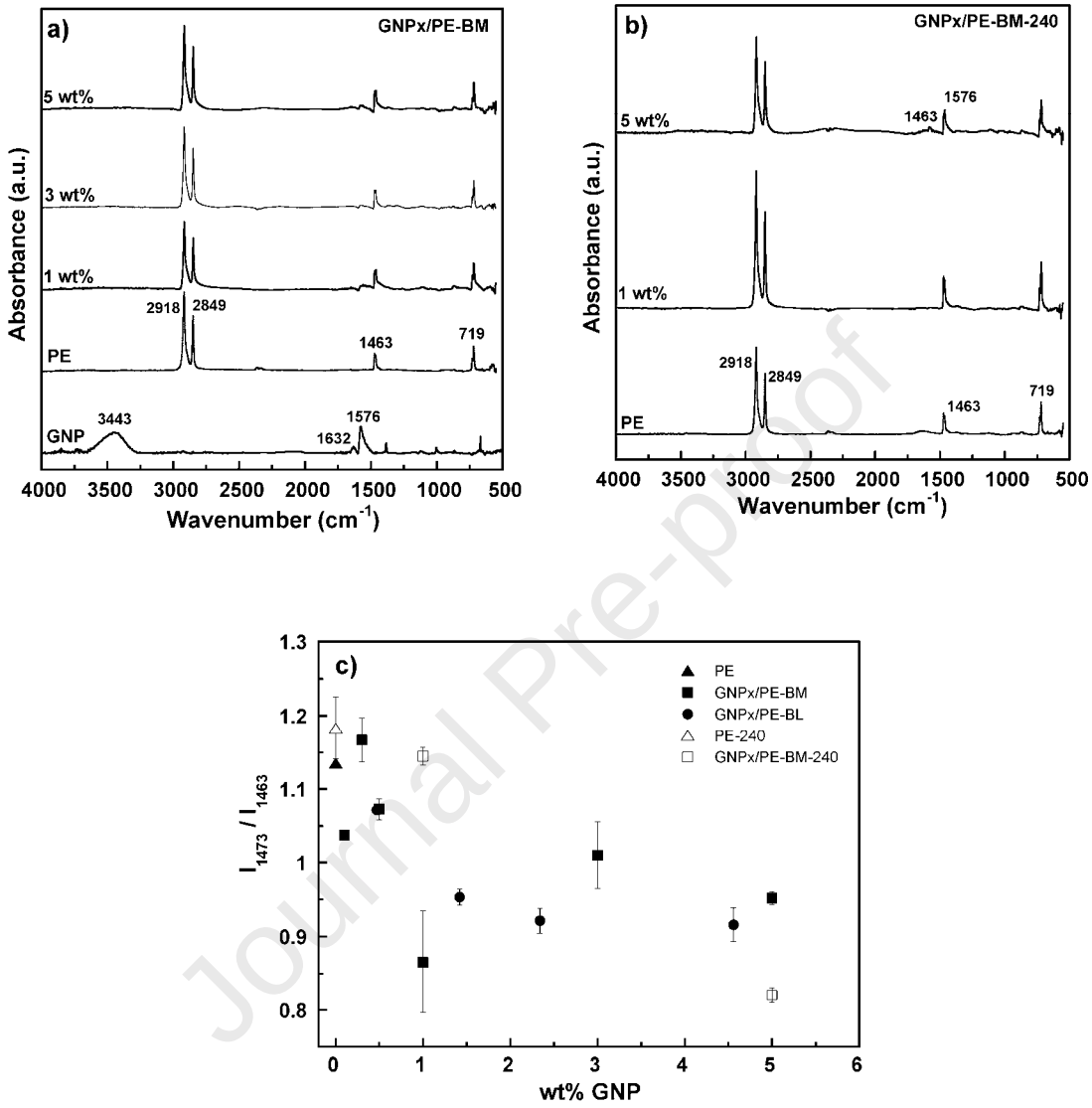

Figure 2.Normalised baseline-subtracted FTIR spectra of GNP, UHMWPE and composites obtained by (a) ball milling and(b) blade mixing;(c) intensity ratio of the methylene bending bands as a function of GNP content and consolidation temperature.

Figure 3 shows the normalised Raman spectra for neat UHMWPE and ball mixed GNPx/UHMWPE composites, all of them consolidated at 175 °C. UHMWPE showed characteristic peaks, as reported previously (Taddei et al., 2002), which include peaks associated with the C–C asymmetric mode at 1060 cm^{-1} and symmetric mode at 1127 cm^{-1}, and other bands due to the -CH_2- twisting vibration at 1293 cm^{-1} and the -CH_2-

bending at 1438 cm^{-1}. On the other hand, Raman spectra of the composites revealed the presence of UHMWPE peaks aforementioned as well as the presence of GNPs via the tangential mode G band for GNPs at around 1580 cm^{-1} and the disorder-induced mode D band at 1345 cm^{-1}.

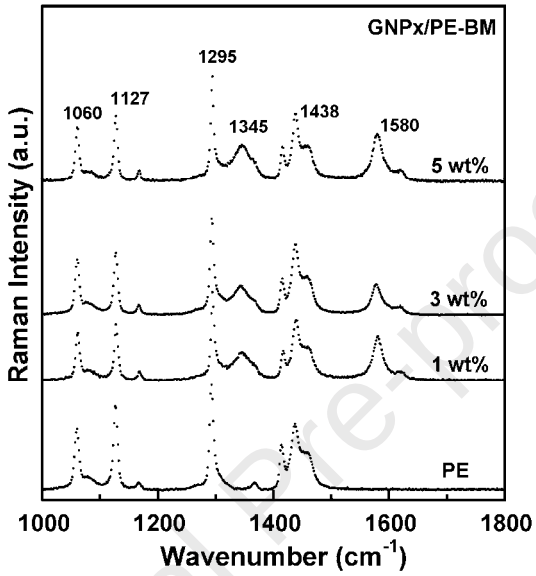

Figure 3. Normalised Raman spectra of UHMWPE and ball mixed GNPx/PE composites consolidated at 175 °C.

3.3 Morphology of the composite coating: freeze-fractured samples

With the aim of studying the coating morphology and coating-substrate adhesion, we analysed SEM micrographs of freeze-fractured surfaces of the composites. Figure 4 shows low magnification images (x100) for these composites.

Considering the composites obtained by ball milling and thermoformed at 175 °C, their micrographs strongly differ as a function of GNP content. At the lowest concentration, 0.1 wt% (Figure 4a), the composite coating had a homogeneous morphology similar to the substrate pattern and showed good adhesion to the UHMWPE matrix, with no signs of delamination. In contrast, for higher filler content, 1 (Figure 4b) and 5 wt% (Figure

4c), two distinct zones can be observed, consisting of a granular morphology and a strong discontinuity associated with the bulk-composite transition. This discontinuity could easily lead to coating delamination. Additionally, bright particles scattered across the composite coating are identified as flake-shaped GNP clusters, in agreement with the findings of Alam et al. (2019). As the filler content increases, the composite maintains a coarse granular morphology and the density of the bright particles increases (Figure 4c). The delamination observed is similar to the phenomenon found by Yilmaz et al. (2019) in materials obtained by injection moulding, but its origin differs. In our case, it is attributable to shear stress during the cooling process, instead of being associated with the interaction between the solidified layer of PE in contact with the mould wall and the highly entangled PE expelled from the nozzle. In contrast, -BL composites (Figures 4e-g) show a more refined grain structure and a smoother transition between bulk and coating, even at filler content of ca. 4.6 wt%, leading to better adhesion in accordance with the observations of Chih et al. (2017).

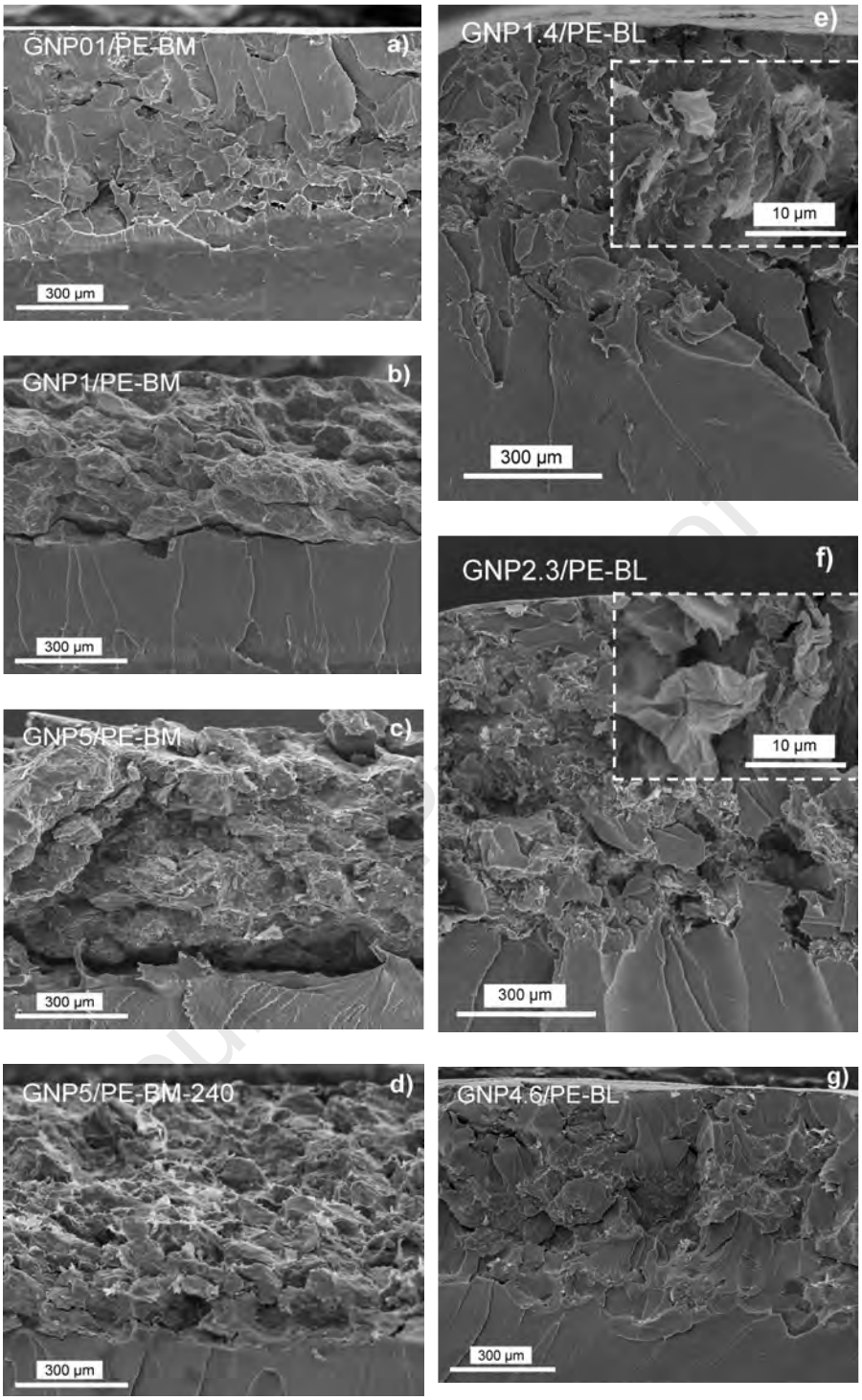

Figure 4. Fractured coatings with different GNP weight concentrations and consolidated at 175 ºC: (a-c) GNPx/PE-BM, (e-g) GNPx/PE-BL, and consolidated at 240 ºC: (d) GNP5/PE-BM-240 ºC.

The poor behaviour of highly filled BM composites can be explained by the presence of numerous GNPs on the surface of polymer powder, which inhibits the consolidation process and results in a segregated structure with a granular size similar to that of the

initial PE powder. This GNP-rich layer interferes in both stages, full wetting followed by complete chain diffusion, as proposed by Gao and Mackley (1994), avoiding a true molecular connectivity between adjacent particles of PE. This necessarily leads to residual voids and localised deformation at original grain boundaries, as suggested by Wu et al. (2002). In contrast, the embedding of GNPs into the void of the fibrillary structure (Figure 1o), avoiding the formation of the segregated structure, provides better adhesion to the PE substrate and a morphology with some signs of ductility. We can understand, in a qualitative way, that the presence of fewer cracks and their smaller size lead to better toughness properties in the -BL than the -BM composites.

Additionally, temperature plays an important role in determining the morphology of the coating layer, refining the granular structure and avoiding the development of a sharp interface between bulk and coating materials, preventing the delamination of the latter. This trend is evidenced in Figure 6d, showing the absence of delamination for the GNP5/PE-BM composite processed at 240 °C.

These results demonstrate that different blending methods and processing temperatures for manufacturing these composite coatings are able to induce strong variations in the uniformity of the layer and the presence of defects, resulting in good adhesion to or delamination from the substrate.

3.4 Microhardness

The hardness of the materials of interest has been influenced by two factors: the mechanical mixing method and the presence of the graphene (Figure 5a). The impact of the first factor is demonstrated by the increases in hardness from 4.15 HV in the neat PE powder in its as-supplied form directly hot pressed to 4.5 HV and 4.75 HV in the PEs

consolidated from the initial powder after using each of the blending techniques studied, i.e., ball mill and blade mixer processes, respectively, this representing increases of 10-15%. The modifications in the PE particles during the mechanical mixing, analysed in Section 3.1, in particular, plastic deformation, might produce this increase in hardness with respect to the thermo-compressed PE.

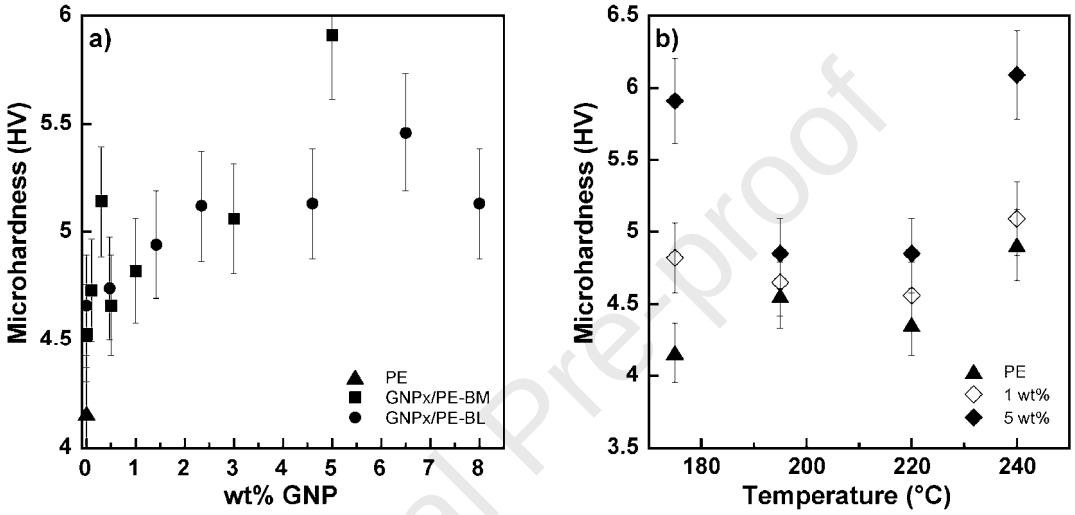

Figure 5. (a) Influence of GNP reinforcement on microhardness for composites processed at 175 °C for BM and BL mixing processes, (b) Change in microhardness with moulding temperature for GNPx/PE-BM (x=0, 1 and 5 wt% GNP content).

The incorporation of GNPs also had a positive influence on hardness. For -BL composites, this increase is monotonous, values approximately stabilising at the highest loading, reaching a hardness of 5.2 HV, this meaning a further 10% increase due to the presence of graphene. In the case of -BM composites, the behaviour is similar above 0.5 wt% GNP content, the difference being that below this critical concentration, there is a relative maximum in hardness at around 5.2 HV, which corresponds to 25% increase with respect to the thermoformed samples containing PE alone. This effect of GNPs on hardness is very high compared to other PE matrix composites reinforced with GO (Colak et al., 2020; Pang et al., 2018; Vadivel et al., 2018), RGO (Colak et al., 2020)

and the same filler GNPs (Aliyu et al., 2019). In general, this effect is explained by an improvement in mechanical response due to load transfer through the filler sheets. In some cases, a relative maximum in hardness is also detected at the lowest filler content, as in Vadivel's study (Vadivel et al., 2018), although with lower intensity. The formation of aggregates around a critical concentration reduces the load transfer, contributing to a local decrease in hardness.

Figure 5b shows the influence of the consolidation temperature on hardness for the neat PE, and GNP1/PE and GNP5/PE composites obtained by ball mill mixing. The main finding is that the use of the highest compression moulding temperature, 240 °C, is positive for all the studied materials, being associated with an increase in hardness with respect to the values at 175 °C, in particular, in neat PE. In general, this increase can be expected to be related to the elimination of fusion defects and the changes produced in the microstructure of the polymer, in particular, the greater crystallinity of the surface coatings. Nonetheless, at intermediate temperatures (195 and 220 °C), the aforementioned positive effect disappears and the hardness is lower for all the materials.

This result cold be due to the increase in ductility found in the neat PE in this temperature range, with its corresponding loss in hardness as consequence of the chain scission increase during the oxidative process as observed by Wu et al. (2002).

3.5 Frictional behaviour

The results describing the changes in the COF as a function of the sliding distance are represented in Figures 6a and 6b for the -BM and -BL composites, respectively. In most cases, the measurements show a running zone, which corresponds to the first 500 m,

followed by a near-stationary value. Figure 6c shows the average COF values obtained in this near-constant zone, from 3000 to 4320 m.

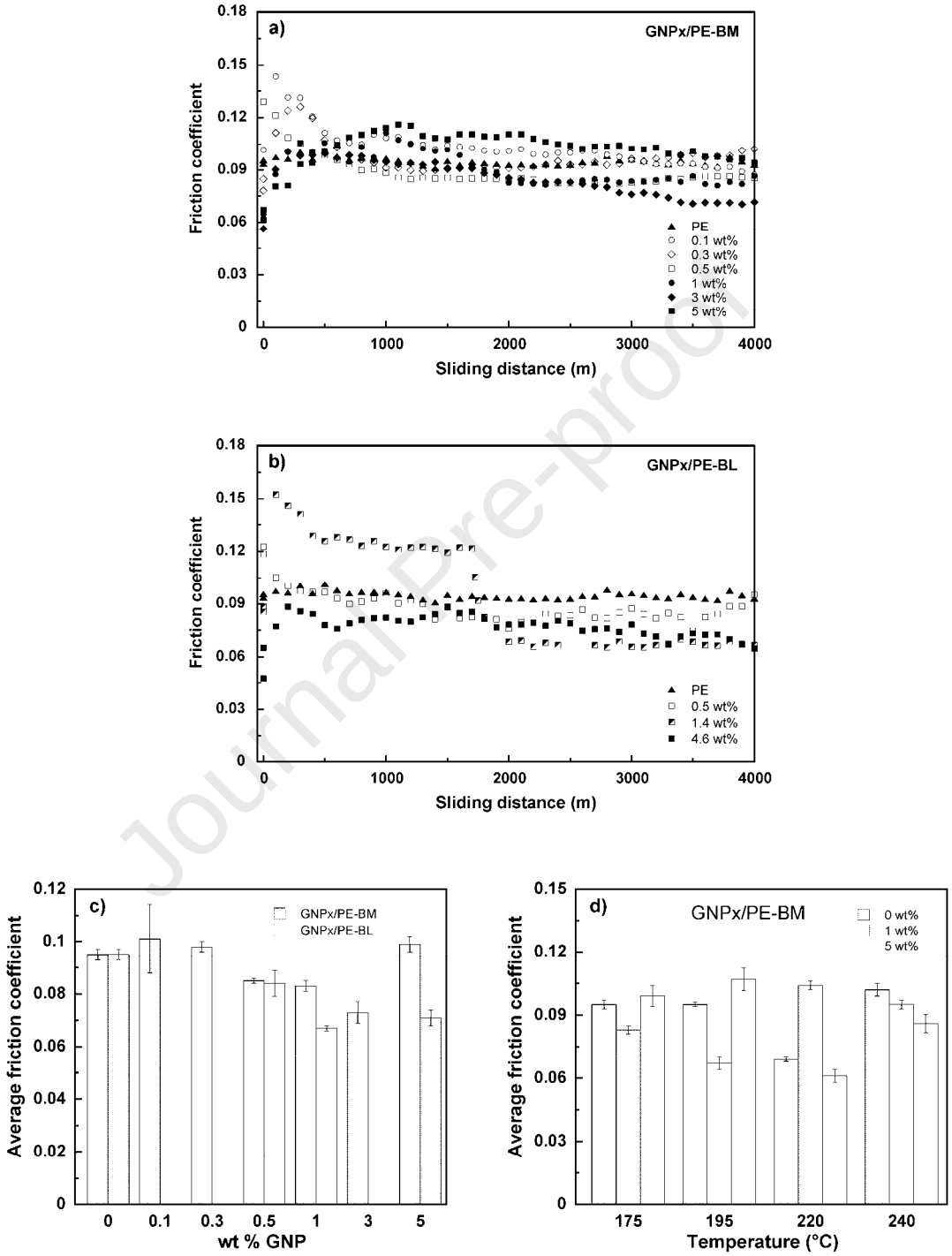

Figure 6. Plots of the coefficient of friction vs. sliding distance for: (a) GNPx/PE-BM and (b) GNPx/PE-BL composites consolidated at 175ºC; average coefficient of friction obtained in the range 3000-400 m as a function of (c) GNP concentration and (d) temperature.

The COF obtained for the neat PE is 0.095 ± 0.002, which is higher than some values obtained previously under similar experimental conditions (Lewis, 1998; Puértolas et al., 2010).

The presence of GNPs in the -BM composites has a positive effect on the COF, although not at all levels of reinforcement. At the lowest GNP content, the effect is practically negligible, the COF remaining unchanged. In contrast, above 0.5 wt%, the lubrication effect of graphene is evidenced, the friction decreasing and reaching a minimum of 0.073 ± 0.004 at 3 wt% GNP content, representing a reduction of 25%. For the -BL composites, the trend is similar, the COF reaching a minimum value of 0.067 ± 0.01 at 1.4 wt%, a reduction of 33% decrease in COF is attributable to the lubrication effect from the interlayer shearing of the multiple layers of the GNP particles, as has also been observed in other studies (Chih et al., 2017; Lahiri et al., 2014), although to a lesser extent.

GNPs do not, however, always have a positive impact on lubrication; for example, a strong increase in COF was observed at 0.5 wt% GNP content (Aliyu et al., 2019). Further, our COF data indicate that at the highest GNP concentrations (above 3 wt%), for both composite families (-BM and -BL), the COF increases further, reaching the value of the neat UHMWPE for the -BM composites, while it is somewhat lower for the -BL ones. This increase could be related to a greater tendency to the formation of aggregates on the surface at these concentrations, which hinder the sliding of the counterpart. A minimum in COF vs GNP content, corresponding to a higher percentage reduction in friction, has also been observed, in an UHMWPE matrix reinforced not only with GNPs, but also with hydroxyapatite nanoparticles at 10 wt% (Taromsari et al., 2019).

The behaviour of the COF as a function of the consolidation temperature, plotted in Figure 6d for PE and the -BM composites at 1 and 5 wt%, is more complex. The neat PE shows a notable decrease in COF (by nearly 25%) at 220 °C, although a further increase (reaching the initial value) is seen at 240 °C. This behaviour is difficult to explain in function of the microstructural changes introduces by the high hot pressed temperatures in the UHMWPE. The increase of polymeric chain mobility generated by the high consolidation temperatures is accompanied by a chain scission du to the oxidative process. The results lead in this temperature region to an increase of the crystallinity with a maximum according to Wu et al. (2002). In our case, the qualitative data of crystallinity deduced from by IR spectra does not show this maximum, but microhardness. However, in general this parameter is more involved in the wear behaviour than in the friction of coefficient. For GNP1/PE-BM composites, the effect of the thermoforming temperature seems to be irrelevant, although a slight increase appears at an intermediate temperature. Finally, at the highest concentration (5 wt%), the influence is uneven with a decrease in COF at 220 °C, but an increase at 240 °C. In this case, the presence of aggregates in the polymer and the free radical scavenger effect of the graphene could be responsible for this complex behaviour.

3.6 Wear behaviour

Morphology of the wear track and counterpart material

Figures 7 and 8 show the SEM images of the wear track after 4320 m of sliding distance for the studied materials and the morphology of the surface of the Al_2O_3 counterpart for representative composites, respectively.

In Figure 7a, the neat PE exhibits a set of grooves oriented parallel to the sliding direction, separated by a few microns, which provides an almost homogeneous morphology at the low magnification (x100). Plastic fragments aligned in the region around some grooves and some small cracks are also observed at the highest magnifications, x5000. This behaviour is associated with an abrasive character and it seems that it is the only wear mechanism acting, since no traces of PE were found on the alumina ball, as seen in Figure 8e. Although water lubrication could prevent the formation of polymer transfer films onto the surface, we will see that this is not always the case for the bearing systems studied.

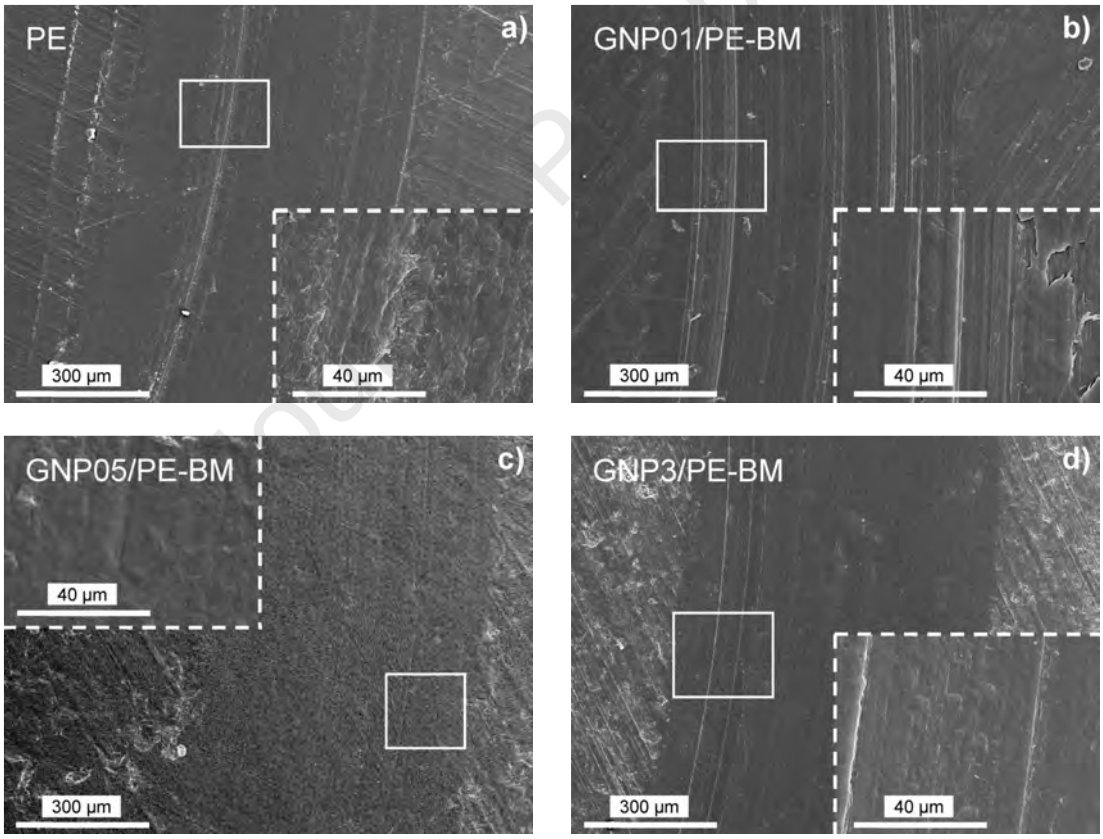

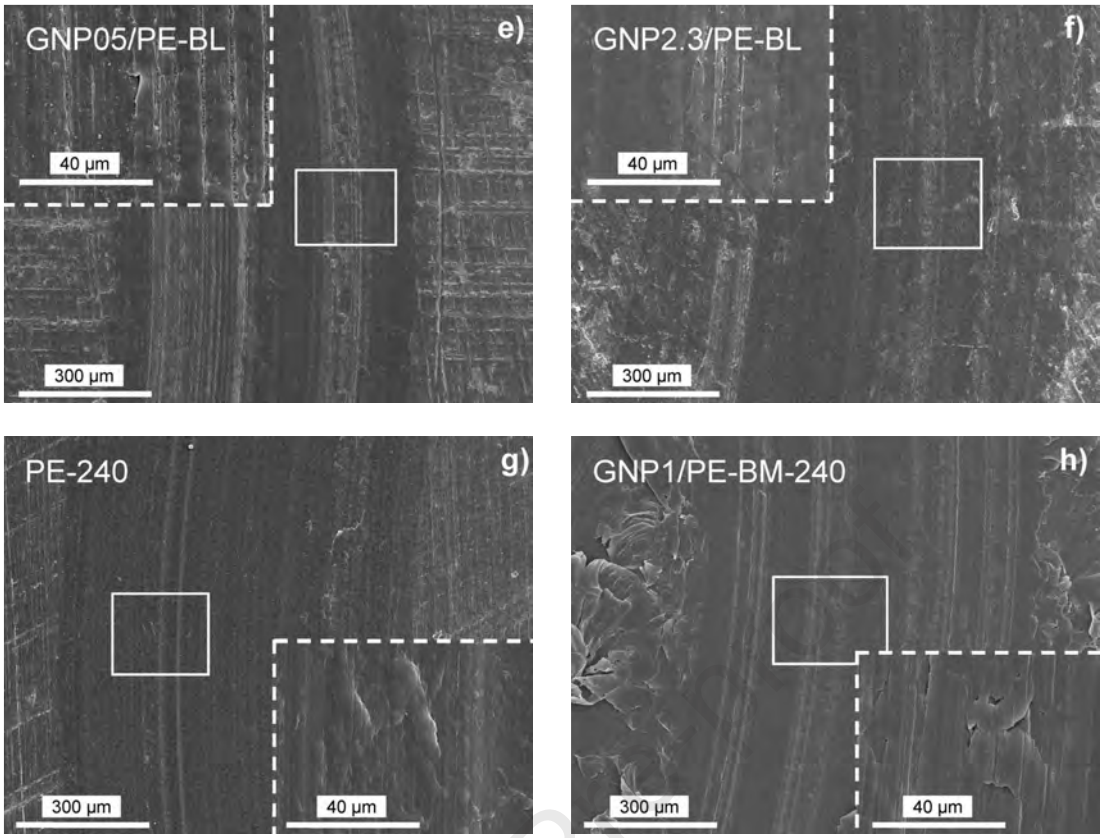

Figure 7. Scanning electron microscopy images of the wear tracks corresponding to: (a) neat PE, (b-d) GNPx/PE-BM, (e-f) GNPx/PE-BL and (g,h) PE and GNP1/PE-BM thermo-compressed at 240 ºC, respectively.

The composite obtained by ball milling with a very small GNP loading (0.1 wt%) had a similar morphology (Fig 7b). Differences include denser, more pronounced grooves, and on the other hand, the image revealed the presence of some eroded film patches, which cover part of the track surface. These films likely reflect a stage in the combined action of abrasive and adhesive wear, which allows layer-by-layer loss of material as has been detected previously in other systems (Kalin et al., 2015; Puértolas et al., 2019). The adhesive wear mechanism is made visible by the presence of several composite scales on the alumina surface (Fig 8a). More qualitative differences are observed in sample GNP05/PE (Figure 7c), on which there are only shallow or practically no signs of abrasive wear, giving rise to a uniform surface on which the mechanisation marks can be seen but are less pronounced than in the zone outside the track. At higher

magnifications, the SEM images reveal a lumpy texture. The first explanation could be associated with a polishing-related effect; however, Figure 8b indicates that composite material was transferred to the ball, in the form of parallel lines of plastic material with some scales, though a smaller quantity than in the case of GNP01/PE composites. In fact, this morphology looks like a negative of the aforementioned pattern formed by the grooves and the patch on GNP01/PE.

In general, at low loadings, the neat PE and the composites show signs of the action of adhesive and abrasive wear mechanisms, the latter reducing their efficacy with GNP content in agreement with the increase in hardness, which reaches a local maximum at 0.5 wt%. At higher concentrations, such as 1 and 3 wt% (Figure 7d), the track surface also appears smooth, although at the highest magnifications the morphology is somewhat lumpy, without sparse grooves but with some bulges, related to the adhesive zones. On the other hand, a significant difference in these composites is the presence of cracks in the sliding direction, which suggests that fatigue wear is involved. Such cracks could be associated with the presence of the GNP aggregates and might be responsible for the loss of toughness observed in the SEM micrographs of freeze-fractured surfaces. For higher filler concentrations, the adhesion mechanism also remains, composite material having been found on the Al_2O_3 ball (Figure 8c). The morphology of the adhesion layer also reflects the lack of a negative replica of the grooves, there being only a few shallow grooves in the wear track consistent with the high hardness. Overall, the analysis of the wear track reveals a transition in the wear behaviour with different mechanisms involved at low and high GNP content similar to that previously observed in RGO/UHMWPE composites (Colak et al., 2020).

In the case of the composites obtained using the blade mixer, -BL, before hot consolidation, the samples with 0.5 and 1 wt% GNP content both have a morphology qualitatively similar to that of the -BM composites with a GNP content below 0.5 wt%, with narrower fringes of grooves surrounded by strong plastic deformation and patches between them. Nonetheless, no longitudinal cracks appear in these composites, implying wear by a combination of abrasive and adhesive mechanisms. Figure 8d shows the effect of the adhesion on the counterpart ball, which has negative grooves and some plastic scales.

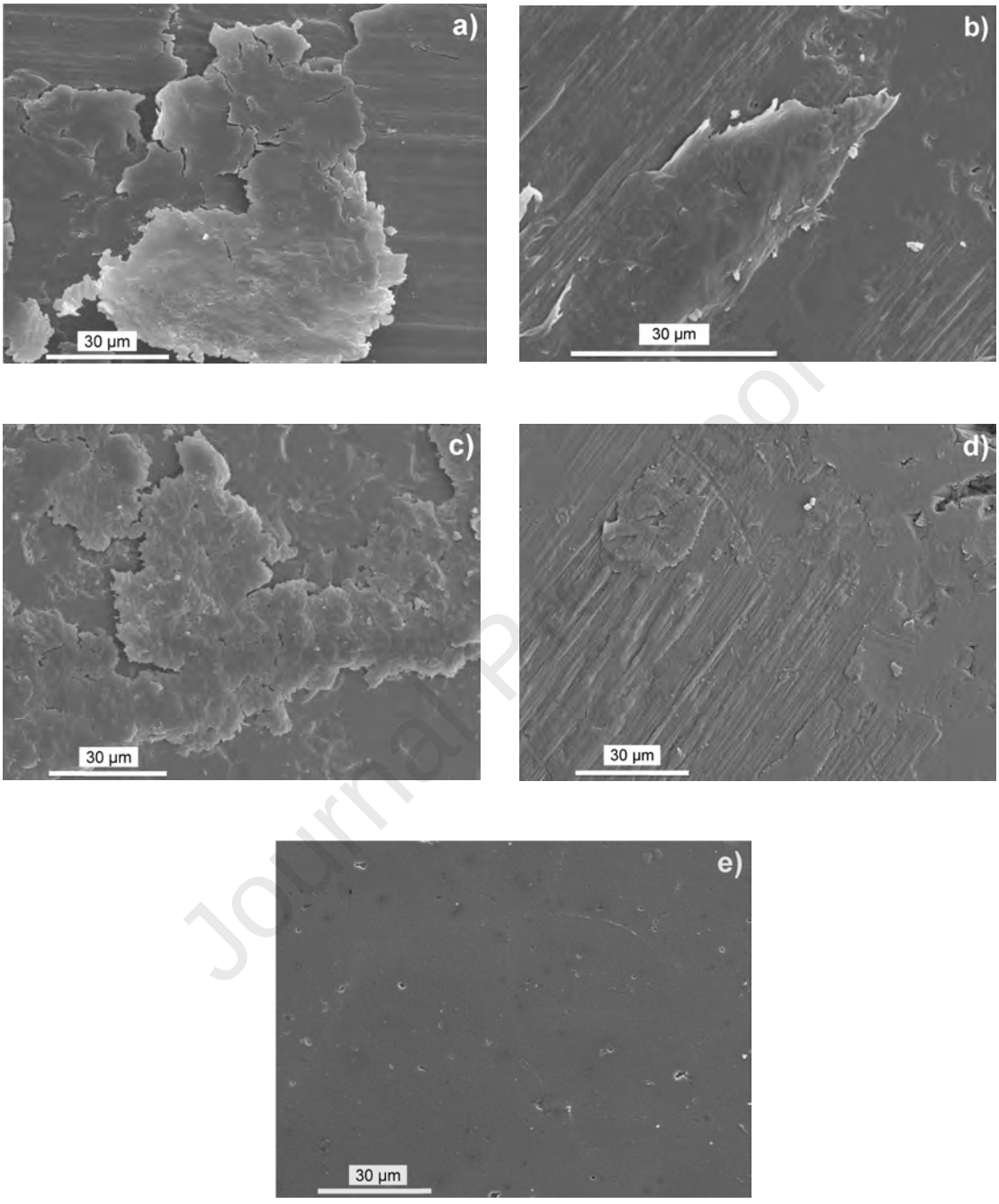

Figure 8. Scanning electron microscopy images of deposited materials on the alumina ball surface after wear testing corresponding to the bearing composites: (a) GNP01/PE-BM, (b) GNP05/PE-BM, (c) GNP1/PE-BM, (d) GNP2.3/PE-BL and (e) neat PE

Finally, the effect of consolidation temperature introduces some changes with respect to the samples manufactured at 175 °C. At 240 °C, a ripple structure appears on the

unfilled PE at high magnifications (Figure 7g), while in GNP1/PE-BM (Figure 7h), a strong plastic deformation accumulates along the edges of the wear track.

Wear track profile

Various different criteria have been reported in the literature for assessing the area A_m of the cross-section of the worn track and consequently the loss of volume. ASTM G99-17 for wear testing with pin-on-disk apparatus provides geometric relationships between this area and the parameters of a circular track. In most wear tests with this kind of counterface geometry (ball-on-disk), however, the shape of the track is far from a circular worn cross-sectional area, as illustrated by the confocal microscopy images of the wear track after 4320 m of sliding distance (Figure 9a). In addition to the track, the area M under the line CC´, which has been used in the literature (Aliyu et al., 2019), the profile also shows a significant lateral increase in area around the ball in some materials, which correspond to the shaded regions BAC and C´A´B´, called L_1 and L_2, respectively. In such cases, in the literature (Lahiri et al., 2014),it is common to use the surface under the line AA´ in order to determine the representative wear area, even though it does not reflect a true loss of material with respect to the unworn line. This option is based on an extended concept of wear, which includes permanent deformation in addition to the loss of material. In this case, this calculation is hindered by the presence of asymmetrical tracks, in which the top of the peaks A and A´ may be very different, as observed in Figure 9a, making it difficult to estimate the area under the line AA´. In this study, we have calculated the values of M and $L=L_1+L_2$ separately, allowing us to calculate M+L as the wear area, which is more accurate than using the area under the line AA´, and additionally, takes into account the material on the edge of

the track. In general, the values of L are the smallest for the composites manufactured using the blade mixer, followed by the composites made by ball milling and the highest for the materials consolidated at the highest temperatures.

In any case, Figure 9b shows that this lateral area is not correlated with microhardness and therefore with plastic deformation. Creep deformation could be the mechanical property involved in the presence of this material above the base line, according to the study of PE acetabular cups of retrieved prostheses (Choudhury et al., 2018; Kumakura et al., 2009). In our opinion, the material at the edges of the wear (Figure 7h) seems more like accumulated material dislodged from the track and then attached to the lateral parts, than a creep effect, although both mechanisms could be operating. Wear rate was calculated by summing the two contributions, M+L, and also by considering only the area M. Since the results were qualitatively the same, as we see in the next paragraph, hereinafter, we will refer to results obtained using M as the wear rates.

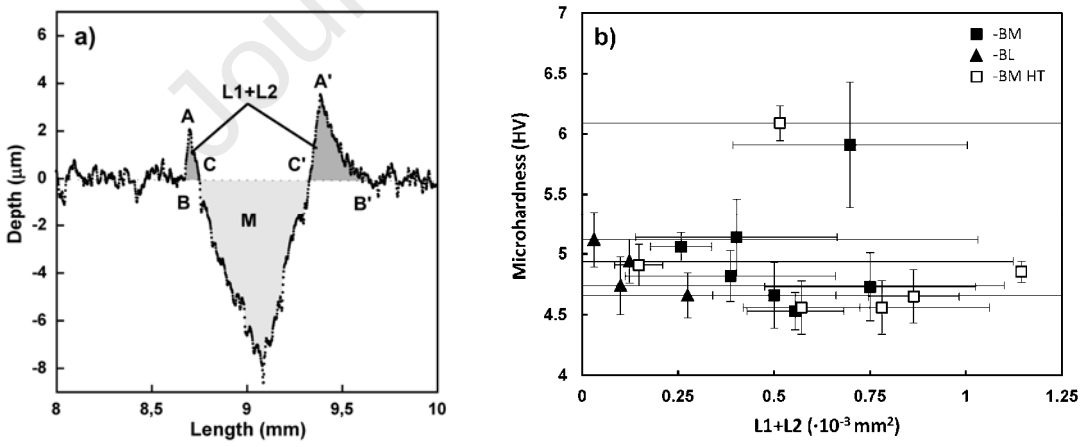

Figure 9. (a) Confocal microscopy image of the worn surface corresponding to GNP1/PE-175-BM after 24 h sliding, (b) Plot of microhardness vs L (L1+L2) for all materials studied.

Wear rate

Figures 10a and 10b indicate the values of k for GNPx/PE-BM and GNPx/PE-BL composites, respectively, estimated from both M and M+L cross-sectional areas of the track. The k_M and k_{M+L} curves for the two types of composite are similar and consequently, as noted above, we focus only on k_M.

The first finding was the difference in wear rate for the neat UHMWPE prepared by each of the blending processes: $20x10^{-7}$ mm^3/Nm in the case of ball milling, consistent with previous data in the literature (Haddadi et al., 2019; Puértolas et al., 2010) for the same experimental conditions and counterpart material, and $37x10^{-7}$ mm^3/Nm for blade mixing. This effect could be related to the powder size of the particle before the hot consolidation, since the only morphological difference observed in the analysis of the particle distribution by SEM was a small thickening of the PE particles when using the blade mixer (Figures 1g and 1i). Although small, this change might be enough to cause an increase in wear rate, this effect having been observed previously with an order of magnitude increase in k when changing from 30 to 140 µm diameter PE particles (Golchin et al., 2016; Vadivel et al., 2018). To our knowledge, no explanation has been given for this correlation between particle size and wear rate. The consolidation defects appearing during the fabrication process as a consequence of the high viscosity of the PE could be the underlying mechanism. Incomplete fusion between PE particles, usually in form of voids (type 1), which disappear at consolidation temperatures above 160 °C, and defects associated with deficiencies in the self-diffusion of the polymer chains between the grains (type 2) are the common defects. These defects are observed by SEM as markings on the surface of fracture samples and the forming the signs of

crack initiation and further propagation under stress, with an influence on ductility and toughness (Gao and Mackley., 1994; Wu et al., 2002).

The higher the PE particle size, the larger the type 2 defects at the boundaries of the original powder particles, this implying that the -BL composites would have lower toughness and loss of wear resistance. Another potentially relevant factor is related to the increase in hardness caused by the mechanical mixing from 4.5 HV for -BM composites to 4.7 HV for the -BL, although these increases seem to be too small to account for the strong changes observed in the PE wear rate.

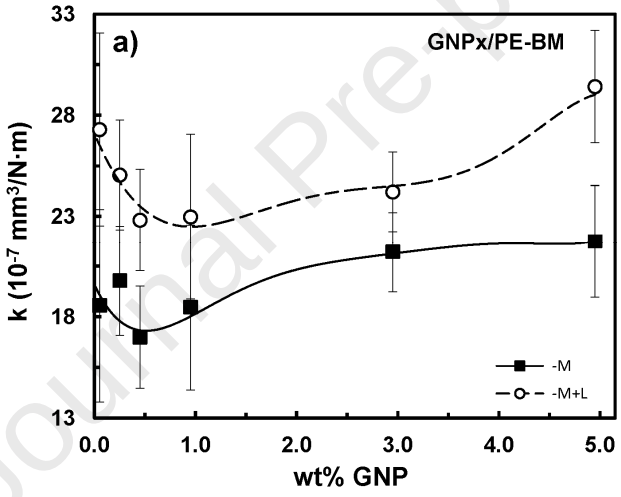

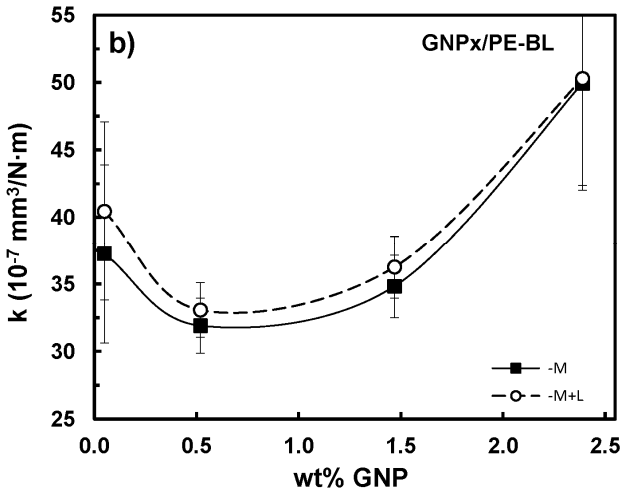

Figure 10. Wear rate calculated after 4320 m of sliding for the composites obtained by both types of mechanical mixing studied followed by a hot compression process at 175 ºC.

The main tribological result for the -BM and -BL composites is that the effect of GNP content is similar in the two families, the k vs GNP content curves showing the same pattern and running almost parallel, maintaining the difference of $15x10^{-7}$ $mm^3/N.m$ with respect to the corresponding unfilled PE. Additionally, we can see that the maximum k intervals generated by the graphene are 18 and $6x10^{-7}$ $mm^3/N.m$ for -BL and -BM composites, respectively, similar values to the effect introduced by the two different mechanical mixing techniques. On the other hand, the main characteristic of the influence of GNP concentration is that a minimum in wear rate appeared at a GNP content of 0.5 wt% in both types of composite, GNPx/PE-BM and GNPx/PE-BL. At this critical concentration, the k value was around 20% and 15% lower than that of the unfilled PE in the first and second family of composites respectively. This behaviour is present in most carbonaceous-based PE composites, like graphite (Lorenzo-Bonet at al., 2019; Pang et al., 2018; Suñer et al., 2018; Vadivel et al., 2018) and RGO (Colak et al., 2020) with reported decreases of 40%, 16%, 30%, 24% and 8% at a filler content 0.1 wt%, 1 wt%, 2 wt%, 1 wt% and 0.7 wt%, respectively. This panoply of results is basically attributable to differences in filler distributions, their intrinsic characteristics and interactions with the PE, as well as in wear testing conditions. Concerning the reinforcement of UHMWPE with GNPs, our data are similar to those in the literature. Specifically, Aliyu's group (Aliyu et al., 2018) found a minimum at 0.25 wt%, with a 33% decrease when the composite was manufactured by hot-pressing and a strong increase in k, by around an order of magnitude, in a composite coating on aluminium prepared by an electrostatic powder spray process. In contrast, Lahiri et al. (2014) found

a monotonous increase in wear resistance with the addition of graphene reinforcement up to 1 wt% using a nanoscale scratch test and calculating the volume removed with the same criterion for the cross-sectional area under the line CC´ as in Figure 9a.

The minimum in wear rate as a function of GNP content has been discussed on the basis that graphene has a high specific surface area which facilitates load transfer in the polymer matrix, in particular, at low filler concentrations where the graphene is well dispersed. This interaction with the polymer makes it difficult for wear mechanisms to remove material during the wear process. Nonetheless, the presence of agglomerated particles at high graphene contents and low dispersion decreases the capability to withstand load transfer and reduces the wear resistance. The similar shape of the k vs GNP content curves, and in particular, the fact that the same wt% value produces the lowest wear rate in both -BM and -BL composites indicate that the appearance of the minimum is related more to the formation of the aggregates than to microstructural changes. Therefore, the modification in the platelet geometry introduced by the blade mixing technique, with the presence of flayed morphology (Figure 1n), in line with other changes observed previously in GNPs due to bent, rolled-up or buckled geometry introduced during fabrication processes (Kalaitzidou et al., 2010), does not seem to be the cause of the minimum in the wear rate.

Another microstructural feature which plausibly may participate in the load transfer is the crystallinity around GNP platelets, as a consequence of a heterogeneous nucleating agent effect during the re-crystallisation process. Nonetheless, the way in which this affects wear rate remains a matter of debate. Specifically, the correlation between crystallinity and wear rate has been considered direct in some UHMWPE-based composites reinforced with graphene-related materials (Pang et al., 2018; Taromsari et

al., 2019), while in others, researchers have observed the opposite trend (Alam et al., 2019; Lorenzo-Bonet at al., 2019) or a strong reduction in wear rate without changes in crystallinity (Golchin et al., 2016). In our -BL materials, the minimum around 1 wt% of the I_{1423}/I_{1463} rate from the IR spectrum (Figure 2c) and consequently the maximum in the degree of crystallinity suggest that these composites follow the second type of trend, while the maximum of peak rate at 0.5 wt% in -BM composites would indicate the first type of correlation.

As hardness and toughness are mechanical parameters involved in wear mechanisms, we should consider how they are influenced by GNP content. Concerning the first property, in -BM composites, hardness seems to be correlated with wear rate, the HV curve having a local minimum at 0.5 wt% followed an increase at higher concentrations and with some fluctuations below this critical content. This correlation was also observed by Vadivel et al. (2018) in graphene-based PE composites, although it is not always present (Aliyu et al., 2019). In GNPx/PE-BL composites, there is no such correlation, the hardness increasing monotonically with GNP concentration, while there is a clear minimum in k at 0.5 wt%. We could conclude that the key factor in hardness is the influence of the presence of graphene, while in wear rate, it is the mechanical mixing technique, as GNPs contribute to the latter tribological property.

Concerning toughness, we do not have direct results for our composites, because the nature of their coating makes it difficult to obtain such data. Nonetheless, the analysis of SEM micrographs of freeze-fractured samples (Figure 4) seems to indicate that the composites become more brittle and less plastic as GNP content increases. On the other hand, it is recognised in the field (Puértolas and Kurtz, 2014) that, in general, a low concentration of graphene fillers helps to enhance toughness, but that above a critical

value, the formation of GNP aggregates decreases toughness as consequence of a stress concentration effect. This correlation between toughness and wear rate is clear in systems with a good aggregation-free dispersion due to the functionalization of the filler (Haddadi et al., 2019). As a result, all this could explain the appearance of the minimum in k and the transition at this concentration from wear governed by adhesion and abrasion mechanisms to a different behaviour where the dominant factors are adhesion and fatigue.

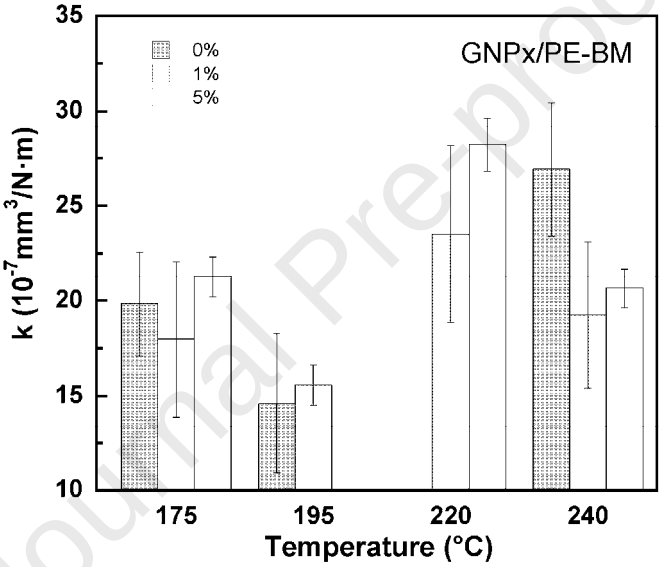

Figure 11. Influence of consolidation temperature on wear rate for composites GNPx/PE-BM with a GNP content of 0, 1 and 5 wt%.

The other processing condition investigated in this study was the use of higher temperatures (from 175 °C up to 240 °C) during the hot-compression moulding. Temperature strongly affects the mobility of the polymer chains, decreasing the reptation time for polymer self-diffusion and contributing to full particle fusion between the grains. The influence of consolidation temperature on wear rate is illustrated in Figure 11. The data indicate a non-monotonic behaviour both in the neat material and in

the composites, with a minimum in the neat PE at intermediate temperatures and a maximum in the composites at the highest GNP concentrations, at approximately the same temperature, around 200-210 °C. Gul et al. (2003) studied the influence of consolidation temperature in the hot-compression process on wear rate at three temperatures (210, 250 and 300 °C) and found no significant differences. On the other hand, Wu et al. (2002) found a maximum in elongation-at-break at around 180 °C when they assessed the influence of consolidation temperature, and explained this in terms of two overlapping phenomena: the highest temperatures reduce consolidation defects leading to an improvement in mechanical properties, in particular, ductility, but simultaneously, the oxidation process at these temperatures leads to a mechanical weakness via chain scission. Graphene, acting as a free radical scavenger (Kolanthai et al., 2015), is able to compensate for the negative effects of the oxidative process at the higher temperatures, and enhance the wear resistance of the composites. This effect is clearly visible in GNP1/PE-BM where at 195 °C the wear rate obtained is 25% lower than that in the neat PE due to the synergy between GNPs and consolidation temperatures. Therefore, the use of the consolidation temperature around 195 ºC allows not only to increase the adhesion of the layer to the substrate according with the figure 4d, but also to enhance the wear resistance of the material. Therefore, the composite material obtained by ball mixing further of thermal process, as bulk material or as coating at concentrations around 0.5 wt% of GNP manufactured by ball mixing decreases the wear rate, at the same time that present a suitable coefficient of friction and hardness.

CONCLUSIONS

GNP/UHMWPE-based composite coatings on UHMWPE substrate were prepared by ball mill and blade mixer techniques followed by thermo-compression at various different moulding temperatures without any GNP functionalization. From a microstructural point of view, ball milling increases the lumpy structure of the PE particles and flakes the GNPs on them, while blade mixing increases the PE particle size and embeds the GNPs into voids in the fibrillary structure. Composite coatings prepared using a blade mixer showed better adhesion to the substrate and higher ductility.

Composites increase the hardness of the hot-pressed powder UHMWPE at the highest concentrations by 24%, due to the GNP contribution and the blending effect on the PE powder. The mixing technique influences wear rate strongly, even more than the presence of graphene. Specifically, composites manufactured by ball milling and further thermo-compression had more wear resistance than those obtained with a blade mixer. Nonetheless, in both composites, a minimum is reached at around 0.5 wt% GNP content. The COF also reached minima at 3 wt% and 1.4 wt%, with strong reductions (by 25% and 33%) in the composites obtained using the ball mill and blade mixer, respectively. On the other hand, no correlations were found with hardness, degree of crystallinity or toughness, the formation of aggregates likely being responsible for these minima.

The effect of consolidation temperature on hardness is weak and almost negligible at the highest GNP content, while it is relevant for the COF in the cases of the neat PE and in composites with lower filler content. Finally, thermoforming at intermediate consolidation temperatures, for example, around 195 °C, enhances wear resistance.

According with the overall results, we can conclude that there is not an optimal GNP for all the properties. From a tribological point of view, 0.5 wt% GNP content would be the better reinforcement to obtain the minimum amount of loss material, suing the ball mill as mechanical mixing technique. Evidently, although the biological activity of the wear debris of this composite material is out of this current work, a minimum wear is positive. On the other hand, the friction coefficient and the hardness, although do not achieve the optimal value, present values, which reduce and increase, respectively, the behaviour of the neat UHMWPE.

ACKNOWLEDGEMENTS

This work has been funded by the Government of Aragon (Spain) together with the European Social Fund (DGA T-48- 17R) and project RIS3:LMP21-18.

REFERENCES

F. Alam, M. Choosri, T.K. Gupta, K.M. Varadarajan, D. Choi, S. Kumar, Electrical, mechanical and thermal properties of graphene nanoplatelets reinforced UHMWPE nanocomposites, Mater Sci Eng B-Adv 241 (2019) 82-91.

I.K. Aliyu, A.S. Mohammed, A. Al-Qutub, Tribological Performance of UHMWPE/GNPs Nanocomposite Coatings for Solid Lubrication in Bearing Applications, Tribol Lett 66(4) (2018).

I.K. Aliyu, A.S. Mohammed, A. Al-Qutub, Tribological Performance of Ultra High Molecular Weight Polyethylene Nanocomposites Reinforced with Graphene Nanoplatelets, Polym Composite 40 (2019) E1301-E1311.

I.K. Aliyu, M.U. Azam, D.U. Lawal, M.A. Samad, Optimization of SiC Concentration and Process Parameters for a Wear-Resistant UHMWPE Nancocomposite, Arab J Sci Eng 45(2) (2020) 849-860.

M.H. Al-Saleh, Electrical and electromagnetic interference shielding characteristics of GNP/UHMWPE composites, J Phys D Appl Phys 49(19) (2016).

D. Berman, A. Erdemir, A.V. Sumant, Graphene: a new emerging lubricant, Mater Today 17(1) (2014) 31-42.

A. Chih, A. Anson-Casaos, J.A. Puértolas, Frictional and mechanical behaviour of graphene/UHMWPE composite coatings, Tribol Int 116 (2017) 295-302.

D. Choudhury, M. Ranusa, R.A. Fleming, M. Vrbka, I. Krupka, M.G. Teeter, J. Goss, M. Zou, Mechanical wear and oxidative degradation analysis of retrieved ultra high molecular weight polyethylene acetabular cups, J Mech Behav Biomed 79 (2018) 314-323.

J. Coates, Interpretation of Analytical Chemistry, A Practical Approach, in: R.A. Meyers (Ed.), Encyclopesia of Analytical Chemistry, John Wiley &Sons Ltd, Chichester, 2000, pp. 10815-10837.

A. Colak, M. Goktas, F. Mindivan, Effect of reduced graphene oxide amount on the tribological properties of UHMWPE biocomposites under water-lubricated conditions, Sn Appl Sci 2(3) (2020).

J.H. Du, L. Zhao, Y. Zeng, L.L. Zhang, F. Li, P.F. Liu, C. Liu, Comparison of electrical properties between multi-walled carbon nanotube and graphene nanosheet/high density polyethylene composites with a segregated network structure, Carbon 49(4) (2011) 1094-1100.

J. Fu, B.W. Ghali, A.J. Lozynsky, E. Oral, O.K. Muratoglu, Ultra high molecular weight polyethylene with improved plasticity and toughness by high temperature melting, Polymer 51(12) (2010) 2721-2731.

P. Gao, M.R. Mackley, A General-Model for the Diffusion and Swelling of Polymers and Its Application to Ultra-High Molecular-Mass Polyethylene, P Roy Soc Lond a Mat 444(1921) (1994) 267-285.

A. Golchin, A. Wikner, N. Emami, An investigation into tribological behaviour of multi-walled carbon nanotube/graphene oxide reinforced UHMWPE in water lubricated contacts, Tribol Int 95 (2016) 156-161.

R.M. Gul, F.J. McGarry, C.R. Bragdon, O.K. Muratoglu, W.H. Harris, Effect of consolidation on adhesive and abrasive wear of ultra high molecular weight polyethylene, Biomaterials 24(19) (2003) 3193-3199.

S.A. Haddadi, A.R. Saadatabadi, A. Kheradmand, M. Amini, M. Ramezanzadeh, SiO2-covered graphene oxide nanohybrids for in situ preparation of UHMWPE/GO(SiO2) nanocomposites with superior mechanical and tribological properties, J Appl Polym Sci 136(31) (2019).

H.L. Hu, G. Zhang, L.G. Xiao, H.J. Wang, Q.S. Zhang, Z.D. Zhao, Preparation and electrical conductivity of graphene/ultrahigh molecular weight polyethylene composites with a segregated structure, Carbon 50(12) (2012) 4596-4599.

K. Kalaitzidou, H. Fukushima, L.T. Drzal, A Route for Polymer Nanocomposites with Engineered Electrical Conductivity and Percolation Threshold, Materials 3(2) (2010) 1089-1103.

M. Kalin, M. Zalaznik, S. Novak, Wear and friction behaviour of poly-ether-ether-ketone (PEEK) filled with graphene, WS2 and CNT nanoparticles, Wear 332 (2015) 855-862.

E. Kolanthai, S. Bose, K.S. Bhagyashree, S.V. Bhat, K. Asokan, D. Kanjilal, K. Chatterjee, Graphene scavenges free radicals to synergistically enhance structural properties in a gamma-irradiated polyethylene composite through enhanced interfacial interactions, Phys Chem Chem Phys 17(35) (2015) 22900-22910.

T. Kumakura, L. Puppulin, K. Yamamoto, Y. Takahashi, G. Pezzotti, In-Depth Oxidation and Strain Profiles in UHMWPE Acetabular Cups Non-Destructively Studied by Confocal Raman Microprobe Spectroscopy, J Biomat Sci-Polym E 20(12) (2009) 1809-1822.

S.M. Kurtz, O.K. Muratoglu, M. Evans, A.A. Edidin, Advances in the processing, sterilization, and crosslinking of ultra-high molecular weight polyethylene for total joint arthroplasty, Biomaterials 20 (1999) 1659-1688.

S.M. Kurtz, UHMWPE. Biomaterials Handbook, Elsevier, (2016).

D. Lahiri, F. Hec, M. Thiesse, A. Durygind, C. Zhang, A. Agarwal, Nanotribological behavior of graphene nanoplatelet reinforced ultra high molecular weight polyethylene composites, Tribol Int 70 (2014) 165-169.

C. Lee, X.D. Wei, J.W. Kysar, J. Hone, Measurement of the elastic properties and intrinsic strength of monolayer graphene, Science 321(5887) (2008) 385-388.

G. Lewis, Contact stress at articular surfaces in total joint replacements. Part I: Experimental methods, Bio-Med Mater Eng 8(2) (1998) 91-110.

T. Liu, A. Eyler, W.H. Zhong, Simultaneous improvements in wear resistance and mechanical properties of UHMWPE nanocomposite fabricated via a facile approach, Mater Lett 177 (2016) 17-20.

E. Lorenzo-Bonet, M.A.L. Hernandez-Rodriguez, O. Perez-Acosta, M.A. De la Garza-Ramos, G. Contreras-Hernandez, A. Juarez-Hernandez, Characterization and tribological analysis of graphite/ultra high molecular weight polyethylene nanocomposite films, Wear 426 (2019) 195-203.

O. Maruzhenko, Y. Mamunya, G. Boiteux, S. Pusz, U. Szeluga, S. Pruvost, Improving the thermal and electrical properties of polymer composites by ordered distribution of carbon micro- and nanofillers, Int J Heat Mass Tran 138 (2019) 75-84.

R.H. Olley, I.L. Hosier, D.C. Bassett, N.G. Smith, On morphology of consolidated UHMWPE resin in hip cups, Biomaterials 20(21) (1999) 2037-2046.

H. Pang, T. Chen, G.M. Zhang, B.Q. Zeng, Z.M. Li, An electrically conducting polymer/graphene composite with a very low percolation threshold, Mater Lett 64(20) (2010) 2226-2229.

W.C. Pang, Z.F. Ni, J.L. Wu, Y.W. Zhao, Investigation of tribological properties of graphene oxide reinforced ultrahigh molecular weight polyethylene under artificial seawater lubricating condition, Appl Surf Sci 434 (2018) 273-282.

J.A. Puértolas, V. Martinez-Nogues, M.J. Martinez-Morlanes, M.D. Mariscal, F.J. Medel, C. Lopez-Santos, F. Yubero, Improved wear performance of ultra high molecular weight polyethylene coated with hydrogenated diamond like carbon, Wear 269(5-6) (2010) 458-465.

J.A. Puértolas, S.M. Kurtz, Evaluation of carbon nanotubes and graphene as reinforcements for UHMWPE-based composites in arthroplastic applications: A review, J Mech Behav Biomed 39 (2014) 129-145.

J.A. Puértolas, S.M., Kurtz, UHMWPE Matrix Composites, in: S.M. Kurtz (Ed.), UHMWPE Biomaterials Handbook, Elsevier, Oxford UK, 2016, pp. 269-388.

J.A. Puértolas, M. Castro, J.A. Morris, R. Rios, A. Anson-Casaos, Tribological and mechanical properties of graphene nanoplatelet/PEEK composites, Carbon 141 (2019) 107-122.

R. Siskey, H. Smelt, K. Boon-Ceelen, M.Persson, UHMWPE Homocomposites and Fibers, in: S.M. Kurtz (Ed.), UHMWPE Biomaterials Handbook, Elsevier, Oxford, U.K., 2016.

S. Suñer, N. Emami, Investigation of graphene oxide as reinforcement for orthopaedic applications, Tribology - Materials, Surfaces and Interfaces 8(1) (2014) 1-6.

S. Suñer, N. Gowland, R. Craven, R. Joffe, N. Emami, J.L. Tipper, Ultrahigh molecular weight polyethylene/graphene oxide nanocomposites: Wear characterization and biological response to wear particles, J Biomed Mater Res B 106(1) (2018) 183-190.

J.A. Szivek, P.L. Anderson, J.B. Benjamin, Average and peak contact stress distribution evaluation of total knee arthroplasties, J Arthroplasty 11(8) (1996) 952-963.

P. Taddei, S. Affatato, C. Fagnano, B. Bordini, A. Tinti, A. Toni, Vibrational spectroscopy of ultra-high molecular weight polyethylene hip prostheses: influence of the sterilisation method on crystallinity and surface oxidation, J Mol Struct 613(1-3) (2002) 121-129.

S.M. Taromsari, M. Salari, R. Bagheri, M.A.F. Sani, Optimizing tribological, tensile & in-vitro biofunctional properties of UHMWPE based nanocomposites with simultaneous incorporation of graphene nanoplatelets (GNP) & hydroxyapatite (HAp) via a facile approach for biomedical applications, Compos Part B-Eng 175 (2019).

S.N. Tripathi, G.S.S. Rao, A.B. Mathur, R. Jasra, Polyolefin/graphene nanocomposites: a review, Rsc Adv 7(38) (2017) 23615-23632.

H.S. Vadivel, A. Golchin, N. Emami, Tribological behaviour of carbon filled hybrid UHMWPE composites in water, Tribol Int 124 (2018) 169-177.

B.J. Wang, H.Y. Li, L.Z. Li, P. Chen, Z.B. Wang, Q. Gu, Electrostatic adsorption method for preparing electrically conducting ultrahigh molecular weight polyethylene/graphene nanosheets composites with a segregated network, Compos Sci Technol 89 (2013) 180-185.

Y.Q. Wang, J.F. Yang, S.Y. Zhou, W.T. Zhang, R. Chuan, Electrical properties of graphene nanoplatelets/ultra-high molecular weight polyethylene composites, J Mater Sci-Mater El 29(1) (2018) 91-96.

J.J. Wu, C.P. Buckley, J.J. O'Connor, Mechanical integrity of compression-moulded ultra-high molecular weight polyethylene: effects of varying process conditions, Biomaterials 23(17) (2002) 3773-3783.

G. Yilmaz, T. Ellingham, L.S. Turng, Injection and injection compression molding of ultra-high-molecular weight polyethylene powder, Polym Eng Sci 59 (2019) E170-E179.

G. Zerbi, G. Gallino, N. Delfanti, L. Baini, Structural Depth Profiling in Polyethylene Films by Multiple Internal-Reflection Infrared-Spectroscopy, Polymer 30(12) (1989) 2324-2327.

H.X. Zhu, Zhiping.; Xie, D.; Fang, Y., Graphene. Fabrication, characterization, properties and applications, Academic Press, 2018.

Highlights

1) GNP/UHMWPE coatings were prepared by diverse mixing and temperature conditions.

2) Consolidation temperature around 195ºC improves the wear rate at low GNP content.

3) Mixing methods and GNP content provide an increase in hardness by 24% respect to PE.

4) GNP introduces a minimum in COF with both techniques with reductions by around 30%.

5) Mixing and GNP content influenced the wear rate, providing a minimum at 0.5 wt%.

Declaration of interests

☐ The authors declare that they have no known competing financial interests or personal relationships that could have appeared to influence the work reported in this paper.

☐The authors declare the following financial interests/personal relationships which may be considered as potential competing interests: